

## HIGH-RESOLUTION IMAGES OF ORBITAL MOTION IN THE TRAPEZIUM CLUSTER: FIRST SCIENTIFIC RESULTS FROM THE MULTIPLE MIRROR TELESCOPE DEFORMABLE SECONDARY MIRROR ADAPTIVE OPTICS SYSTEM<sup>1</sup>

LAIRD M. CLOSE,<sup>2</sup> FRANCOIS WILDI,<sup>2</sup> MICHAEL LLOYD-HART,<sup>2</sup> GUIDO BRUSA,<sup>2,3</sup> DON FISHER,<sup>2</sup> DOUG MILLER,<sup>2</sup>  
ARMANDO RICCARDI,<sup>3</sup> PIERO SALINARI,<sup>3</sup> DONALD W. MCCARTHY,<sup>2</sup> ROGER ANGEL,<sup>2</sup> RICH ALLEN,<sup>2</sup>  
H. M. MARTIN,<sup>2</sup> RICHARD G. SOSA,<sup>2</sup> MANNY MONTOYA,<sup>2</sup> MATT RADEMACHER,<sup>2</sup> MARIO RASCON,<sup>2</sup>  
DYLAN CURLEY,<sup>2</sup> NICK SIEGLER,<sup>2</sup> AND WOLFGANG J. DUSCHL<sup>4</sup>

*Received 2003 June 24; accepted 2003 August 13*

### ABSTRACT

We present the first scientific images obtained with a deformable secondary mirror adaptive optics (AO) system. We utilized the 6.5 m Multiple Mirror Telescope adaptive optics system to produce high-resolution (FWHM = 0".07) near-infrared (1.6  $\mu\text{m}$ ) images of the young ( $\sim 1$  Myr) Orion Trapezium  $\theta^1$  Ori cluster members. A combination of high spatial resolution and high signal-to-noise ratio allowed the positions of these stars to be measured to within  $\sim 0".003$  accuracies. We also present slightly lower resolution (FWHM  $\sim 0".085$ ) images from Gemini with the Hokupa'a AO system as well. Including previous speckle data from Weigelt et al., we analyze a 6 yr baseline of high-resolution observations of this cluster. Over this baseline we are sensitive to relative proper motions of only  $\sim 0".002$  yr<sup>-1</sup> (4.2 km s<sup>-1</sup> at 450 pc). At such sensitivities we detect orbital motion in the very tight  $\theta^1$  Ori B2-B3 (52 AU separation) and  $\theta^1$  Ori A1-A2 (94 AU separation) systems. The relative velocity in the  $\theta^1$  Ori B2-B3 system is  $4.2 \pm 2.1$  km s<sup>-1</sup>. We observe  $16.5 \pm 5.7$  km s<sup>-1</sup> of relative motion in the  $\theta^1$  Ori A1-A2 system. These velocities are consistent with those independently observed by Schertl et al. with speckle interferometry, giving us confidence that these very small ( $\sim 0".002$  yr<sup>-1</sup>) orbital motions are real. All five members of the  $\theta^1$  Ori B system appear likely gravitationally bound (B2-B3 is moving at  $\sim 1.4$  km s<sup>-1</sup> in the plane of the sky with respect to B1, where  $V_{\text{esc}} \sim 6$  km s<sup>-1</sup> for the B group). The very lowest mass member of the  $\theta^1$  Ori B system (B4) has  $K' \sim 11.66$  and an estimated mass of  $\sim 0.2 M_{\odot}$ . Very little motion ( $4 \pm 15$  km s<sup>-1</sup>) of B4 was detected with respect to B1 or B2; hence, B4 is possibly part of the  $\theta^1$  Ori B group. We suspect that if this very low mass member is physically associated, it most likely is in an unstable (nonhierarchical) orbital position and will soon be ejected from the group. The  $\theta^1$  Ori B system appears to be a good example of a star formation "minicluster," which may eject the lowest mass members of the cluster in the near future. This "ejection" process could play a major role in the formation of low-mass stars and brown dwarfs.

*Subject headings:* binaries: general — instrumentation: adaptive optics — stars: evolution — stars: formation — stars: low-mass, brown dwarfs

*On-line material:* color figures

### 1. INTRODUCTION

The detailed formation of stars is still a poorly understood process. In particular, the formation of the lowest mass stars and brown dwarfs is uncertain. Detailed three-dimensional simulations of star formation by Bate, Bonnell, & Bromm (2002) suggest that stellar embryos form into "miniclusters" that dynamically decay, "ejecting" the lowest mass members. Such theories can explain why there are far more field brown dwarfs (BD) compared to BD companions of solar-type stars (McCarthy, Zuckerman, & Becklin 2003) or early M stars (Hinz et al. 2002). Moreover, these theories, which invoke some sort of dynamical decay (Durisen, Sterzik, & Pickett 2001) or ejection (Reipurth &

Clarke 2001), suggest that there should be no wide ( $>20$  AU), very low mass (VLM;  $M_{\text{tot}} < 0.185 M_{\odot}$ ) binary systems observed. Indeed, the adaptive optics (AO) surveys of Close et al. (2003a) and the *Hubble Space Telescope* surveys of Reid et al. (2001), Burgasser et al. (2003), Bouy et al. (2003), and Gizis et al. (2003) have not discovered any wide ( $>16$  AU) VLM systems of the 34 systems known to date. As well, the dynamical biasing toward the ejection of the lowest mass members naturally suggests that the frequency of VLM binaries should be much less ( $\lesssim 5\%$  for  $M_{\text{tot}} \sim 0.16 M_{\odot}$ ) than for more massive binaries ( $\sim 60\%$  for  $M_{\text{tot}} \sim 1 M_{\odot}$ ). Indeed, observations suggest that the binarity of VLM systems with  $M_{\text{tot}} \lesssim 0.185 M_{\odot}$  is 10%–15% (Close et al. 2003a; Burgasser et al. 2003), which, although higher than predicted, is still lower than that of the  $\sim 60\%$  of G star binaries (Duquennoy & Mayor 1991).

Despite the success of these decay or ejection scenarios in predicting the observed properties of binary stars, it is still not clear that miniclusters even exist in the early stages of star formation. To better understand whether such miniclusters do exist, we have examined the closest major OB star formation cluster for signs of such miniclusters. Here we focus on the  $\theta^1$  Ori stars in the Trapezium cluster. Trying

<sup>1</sup> A portion of the results presented here made use of the of Multiple Mirror Telescope Observatory, a facility jointly operated by the University of Arizona and the Smithsonian Institution.

<sup>2</sup> Steward Observatory, University of Arizona, Tucson, AZ 85721; lclose@as.arizona.edu.

<sup>3</sup> INAF—Osservatorio Astrofisico di Arcetri, Largo Enrico Fermi, I-50125 Florence, Italy.

<sup>4</sup> Institut für Theoretische Astrophysik, Tiergartenstrasse 15, D-69121 Heidelberg, Germany.

to determine whether some of the tight star groups in the Trapezium cluster are gravitationally bound is a first step to determining whether bound miniclusters exist. In particular, we will examine the case of the  $\theta^1$  Ori B and A groups.

The Trapezium OB stars ( $\theta^1$  Ori A, B, C, D, and E) consists of the most massive OB stars located at the center of the Orion Nebula star formation cluster (for a review, see Genzel & Stutzki 1989). Because of the luminous nature of these stars, they have been the target of several high-resolution imaging studies. Utilizing only tip-tilt compensation, McCaughrean & Stauffer (1994) mapped the region at  $K'$  from the 3.5 m Calar Alto telescope. They noted that  $\theta^1$  Ori B was really composed of two components (B1 and B2) about  $\sim 1''$  apart. Higher  $\sim 0''.15$  resolutions were obtained from the same telescope by Petr et al. (1998) with speckle holographic observations. At these higher resolutions Petr et al. (1998) discovered that  $\theta^1$  Ori B2 was really a  $0''.1$  system (B2 and B3) and that  $\theta^1$  Ori A was really a  $\sim 0''.2$  binary (A1 and A2). A large AO survey of the inner 6 arcmin<sup>2</sup> was carried out by Simon, Close, & Beck (1999), who discovered a very faint (100 times fainter than B1) object (B4) located just  $0''.6$  between B1 and B2. Moreover, a spectroscopic survey (Abt, Wang, & Cardona 1991) showed that B1 was really an eclipsing spectroscopic binary (B1 and B5; separation 0.13 AU; period 6.47 days). In addition,  $\theta^1$  Ori A1 was also found to be a spectroscopic binary (A1 and A3; separation 1 AU; Bossi et al. 1989). Weigelt et al. (1999) carried out bispectrum speckle interferometric observations at the larger Russian Special Astrophysical Observatory (SAO) 6 m telescope (two runs in 1997 and 1998). These observations showed  $\theta^1$  Ori C was a very tight  $0''.033$  binary. These observations also provided the first set of accurate relative positions for these stars. Schertl et al. (2003) have continued to monitor this cluster of stars and have independently detected an orbital motion ( $\Delta P.A. \sim 6^\circ$  for  $\theta^1$  Ori A2 around A1 and  $\Delta P.A. \sim 8^\circ$  for  $\theta^1$  Ori B3 around B2 over a 5.5 yr baseline). They conclude that this is real orbital motion. We present additional recent AO observations of these binaries as an independent check to confirm that these motions are indeed real.

We first utilized the Gemini telescope (with the Hokupa'a AO system) and then observed  $\theta^1$  Ori B during the commissioning of the world's first secondary deformable mirror at the 6.5 m Multiple Mirror Telescope (MMT). In this paper we outline how the observations were carried out and how the stellar positions were measured. We fit the observed positions to calculate velocities (or upper limits) for the  $\theta^1$  Ori B and A stars. In agreement with Schertl et al. (2003), we find that there is good evidence that the  $\theta^1$  Ori B group may be a bound "minicluster" and that the  $\theta^1$  Ori A group is also likely gravitationally bound.

## 2. OBSERVATIONS

We have utilized the University of Arizona adaptive secondary AO system to obtain the most recent high-resolution images of the young stars in the Trapezium cluster (the  $\theta^1$  Ori group).

### 2.1. The World's First Adaptive Secondary AO System Scientific Results

The 6.5 m MMT telescope has a unique adaptive optics system. To reduce the aberrations caused by atmospheric

turbulence, all AO systems have a deformable mirror that is updated in shape at  $\sim 500$  Hz (Close 2000, 2003). Until now, all adaptive optics systems have located this deformable mirror (DM) at a reimaged pupil (effectively a compressed image of the primary mirror). To reimage the pupil onto a DM typically requires 6–8 warm additional optical surfaces, which significantly increase the thermal background and decrease the optical throughput of the system (Lloyd-Hart 2000). However, the MMT utilizes a completely new type of DM. This DM is both the secondary mirror of the telescope and the DM of the AO system. In this manner there are no additional optics required in front of the science camera. Hence, the emissivity is lower, and the possibility of thermal IR AO imaging (Close et al. 2003b; Biller et al. 2003) becomes a reality.

The DM consists of 336 voice coil actuators that push on 336 small magnets glued to the back surface of a thin (2.0 mm thick) 642 mm aspheric ultralow expansion glass "shell" (for a detailed review of the secondary mirror, see Brusa et al. 2003). We have complete positional control of the surface of this reflective shell by use of a capacitive sensor feedback loop. This positional feedback loop allows one to position an actuator of the shell to within 4 nm rms (total surface errors amount to only 40 nm rms over the whole secondary). The AO system samples at 550 Hz using 108 active subapertures. For a detailed review of the MMT AO system see Wildi et al. (2003 and references within).

### 2.2. MMT AO Observations

During our second engineering run we observed the  $\theta^1$  Ori B group on the night of 2003 January 20 (UT). The AO system corrected the lowest 52 system modes and was updated at 550 Hz. The closed-loop bandwidth was estimated at 20 Hz 0 dB. Without AO correction our images had FWHM =  $0''.6$ ; after AO correction our 23 s images had improved to FWHM =  $0''.070$  (close to the diffraction limit of  $0''.056$  in the  $H$  band). A detailed analysis suggested that during our engineering run, a 20 Hz vibration in the MMT telescope increased our FWHM by  $\sim 0''.015$  and decreased our Strehl by a factor of 2. We are in the process of decreasing the effect of this 20 Hz vibration. In any case, as Figure 1 clearly shows, there is a large improvement in image quality (the Strehl increases by 20 times) with the adaptive secondary AO system.

#### 2.2.1. The Indigo Near-IR Video Camera

Since these observations were carried out during the engineering run, we utilized a commercially available  $320 \times 256$  InGaAs 0.9–1.68  $\mu\text{m}$  "Merlin-NIR" video camera. Although this commercial camera (produced by the Indigo company) is not nearly as sensitive as our facility AO camera (AIRES; McCarthy et al. 1998), it still provides excellent dynamical information about the performance of the AO system on bright objects (it was replaced by the ARIES camera in the fall of 2003). Here we use it as a simple NIR ( $H$ -band) science camera.

The Indigo camera was fed by a relay lens that converted the  $f/15$  AO corrected beam to an  $f/39$  beam, yielding  $0''.0242 \pm 0''.0020$  pixel<sup>-1</sup> (providing a  $7''.7 \times 6''.2$  field of view [FOV]). Astrometric standards ADS 8939 and ADS 7158 were observed to calibrate this plate scale and error (see Figs. 2 and 3). It was found that the direction of north was slightly ( $0^\circ.113$ ) east of Indigo's  $Y$ -axis (when the paral-

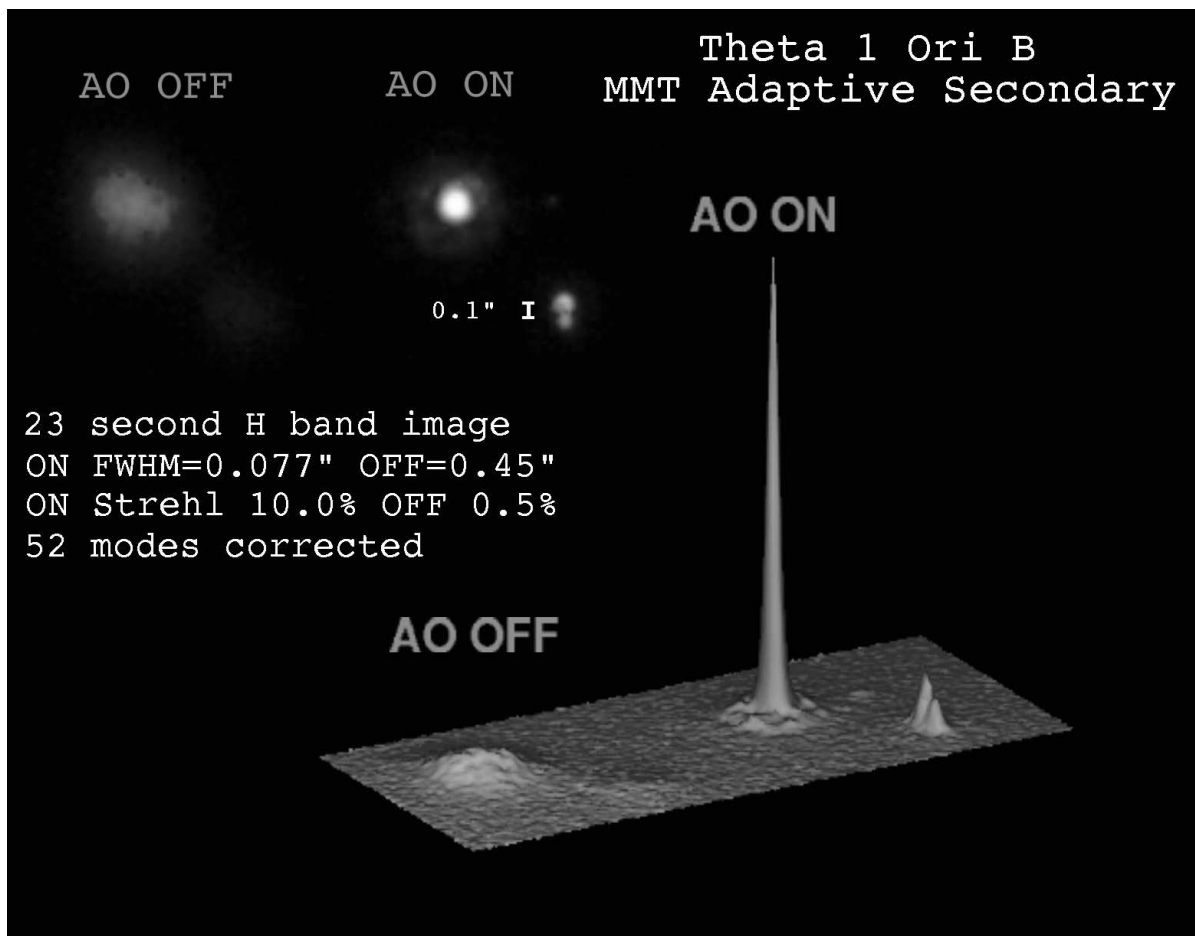


FIG. 1.—Typical example of how the MMT AO system can make very sharp images. With AO “off”  $\theta^1$  Ori B appears to be just two stars. With AO turned “on” it is clearly a tight group of four visual stars. Note how with AO correction the peak intensity increases by 20 times and the resolution becomes 10 times better. [See the electronic edition of the Journal for a color version of this figure.]

lactic angle was zero [transit] and one is looking toward the south). During this commissioning run we did not observe with the MMT Cassegrain derotator tracking field rotation; hence, all images must be rotated by the appropriate parallactic angle (plus an additional  $+0^\circ.113$ ) to have north up and east to the left on the Indigo camera.

The camera was mounted under a high optical quality dichroic that reflected the visible light ( $0.5\text{--}1\ \mu\text{m}$ ) to the 108 subaperture Shack-Hartmann wave front sensor (WFS). The infrared light ( $\lambda > 1\ \mu\text{m}$ ) was transmitted to the Indigo camera. The camera had a standard *H*-band filter ( $1.6\ \mu\text{m}$ ) mounted 3 inches from focus in a light-tight barrel.

To maximize the sensitivity of the Indigo camera, we carried out a standard “two-point” calibration on a both a dark (cold) flat-field source and on a bright (hot) source to scale the automatic gain control/dynamic range of the camera’s electronics. This appeared to yield images that were auto-flat-fielded to a few percent in accuracy when the counts were between the linear range defined by the dark and bright calibration flats. The camera was remotely controlled via a serial port. Digital (16-bit) data were streamed to the control PC’s hard drive. Data could be acquired as fast as  $50\ \text{frames s}^{-1}$  (although data in this paper were acquired at  $15\ \text{frames s}^{-1}$  to sample longer periods on the sky). Integration times can range from 1 to  $16,000\ \mu\text{s}$ . The lack of a longer integration time (since the camera is primar-

ily intended for commercial high-background, high-bandwidth applications) leads to most sources being read-noise limited. However, we found that point sources of  $H \sim 11$  could be detected in 3 s of total exposure (200 16 ms frames) with AO correction at the MMT. Although insensitive by most astronomical standards, the Indigo camera is able to capture temporal events of durations as short as  $1\ \mu\text{s}$ . In this paper we will focus on the ability of the Indigo camera to produce high-resolution ( $0''.07$ ) images of the  $\theta^1$  Ori B group.

#### 2.2.2. Reducing the Indigo MMT AO Data

For the  $\theta^1$  Ori B group we obtained seven series of  $200 \times 16$  ms data cubes with the Indigo camera (not speckle processed). The data from each cube were simply averaged together to produce seven individual 3.2 s exposures. A similarly reduced cube of “sky” images was subtracted from each data set. These seven sky-subtracted exposures were then rotated (in IRAF) by the current parallactic angle (plus the  $0^\circ.113$  offset), so that north was aligned with the *Y*-axis, and east is the negative *X*-axis. Then each of the seven images were cross-correlated and aligned with a cubic spline interpolator. Then, the final stack of images were median-combined to produce the final image. The final image is displayed in Figure 4.

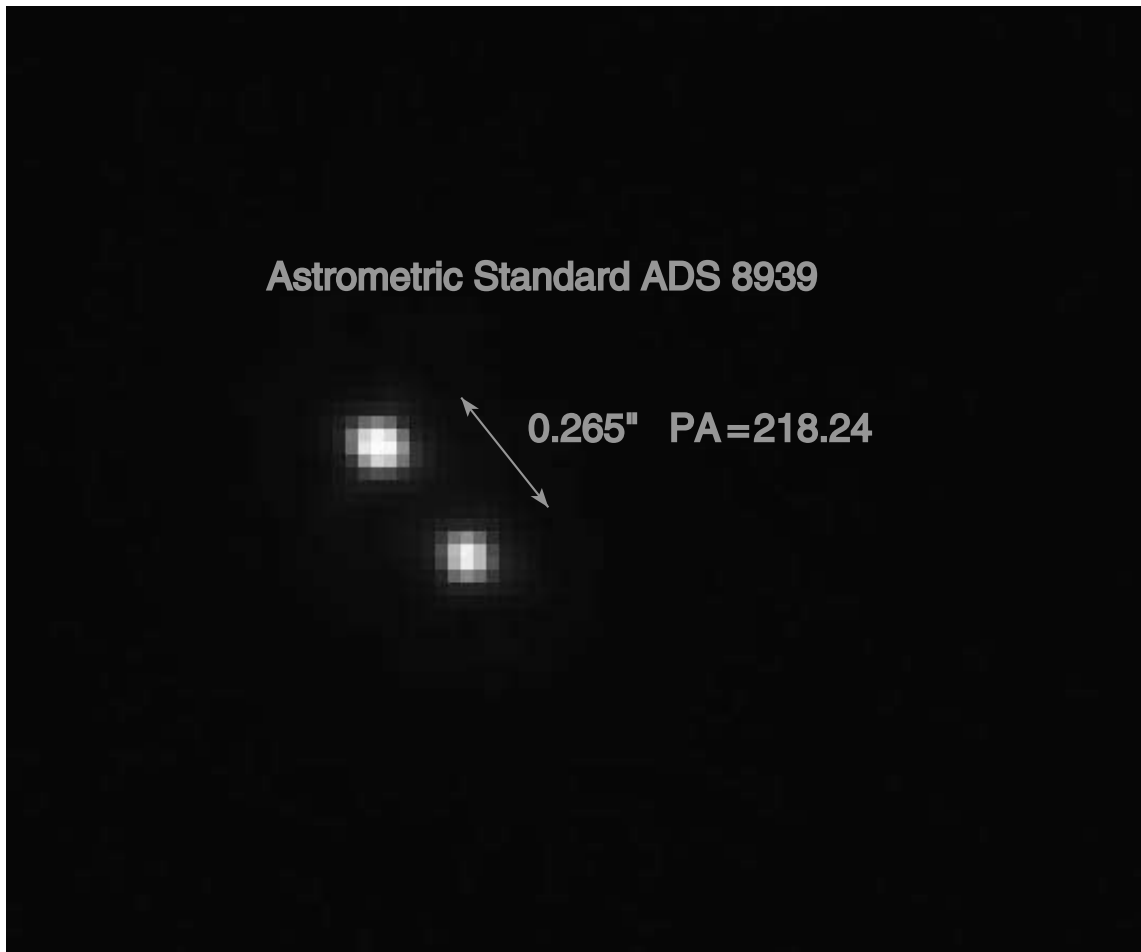


FIG. 2.—*H*-band MMT AO image of the astrometric binary ADS 8939 (WDS 13329+3454; STT 269AB). The well-known orbit (WDS grade level 2) of this binary star predicted a separation of  $0''.265$  and a P.A. of  $218^\circ.237$  for 2003 January 19 UT (the night of this observation). For these values we derived that the Indigo camera had a plate scale of  $0''.0242 \text{ pixel}^{-1}$ . This 10 s integration had a midpoint time of 12:21:30 UT; hence, the parallactic angle during this exposure was  $-107^\circ.6$ . Rotating the image by  $-107^\circ.6$  (clockwise) resulted in a measured P.A. of  $218^\circ.35$ , which indicates that north is  $0^\circ.113$  east of the Indigo's *Y*-axis. Color scale is linear. North is up, and east is to the left. [See the electronic edition of the *Journal* for a color version of this figure.]

### 2.3. Hokupa'a/Gemini Images of the Trapezium

In addition to our excellent MMT images of the  $\theta^1$  Ori B group we also have an epoch of *K'* images of the central  $30''$  of the cluster. These Hokupa'a/Gemini (Graves et al. 1998; Close et al. 1998) AO images were taken 2001 September 19. We acquired a series of 10 short (1 s) images and dithered the telescope in a  $10'' \times 10''$  box, while AO-guiding on  $\theta^1$  Ori B itself (as in the case of the MMT AO observations). We utilized the QUIRC IR camera (Hodapp et al. 1996) with a calibrated plate scale of  $0''.0199 \pm 0''.0002 \text{ pixel}^{-1}$  (Potter et al. 2002).

#### 2.3.1. Reducing the Gemini Data

We have developed an AO data reduction pipeline in the IRAF language that maximizes sensitivity and image resolution. This pipeline is standard IR AO data reduction and is described in detail in Close et al. (2002a, 2002b).

The pipeline cross-correlates and aligns each image, then rotates each image so that north is up (to an accuracy of  $\pm 0^\circ.3$ ) and east is to the left, then median-combines the data with an average sigma clip rejection at the  $\pm 2.5 \sigma$  level. With the use of a cubic-spline interpolator, the script preserves image resolution to a less than 0.02 pixel level. Next, the

custom IRAF script produces two final output images, one that combines all the images taken (see Fig. 5) and another in which only the sharpest 50% of the images are combined (this high-Strehl image was very similar to that shown in Fig. 5, just a bit noisier—and so was not further analyzed).

The final image (see Figs. 5 and 6) has  $\text{FWHM} = 0''.085$ , which is just slightly worse than the MMT data. Even though Gemini is a larger telescope (8.2 m), Hokupa'a's fitting error (36 elements over  $50 \text{ m}^2$ ) is worse than that of the MMT (52 modes over  $33 \text{ m}^2$ ); hence, higher resolution images can result from the smaller of the two telescopes (Gemini has a diffraction limit of  $0''.056$  at *K'* similar to that of the MMT at *H*). However, Hokupa'a's curvature WFS could guide on much fainter ( $R \sim 17$ ) guide stars (Close et al. 2002a, 2002b; Siegler, Close, & Freed 2003).

## 3. REDUCTIONS

In Table 1 we present the analysis of our MMT and Gemini images in Figures 4 and 5. The photometry was based on DAOPHOT's point-spread function (PSF) fitting photometry task ALLSTARS (Stetson 1987). The PSF used was  $\theta^1$  Ori B1 itself. Since all the members of the  $\theta^1$  Ori B group are located within  $1''$  of  $\theta^1$  Ori B1, the PSF fit is

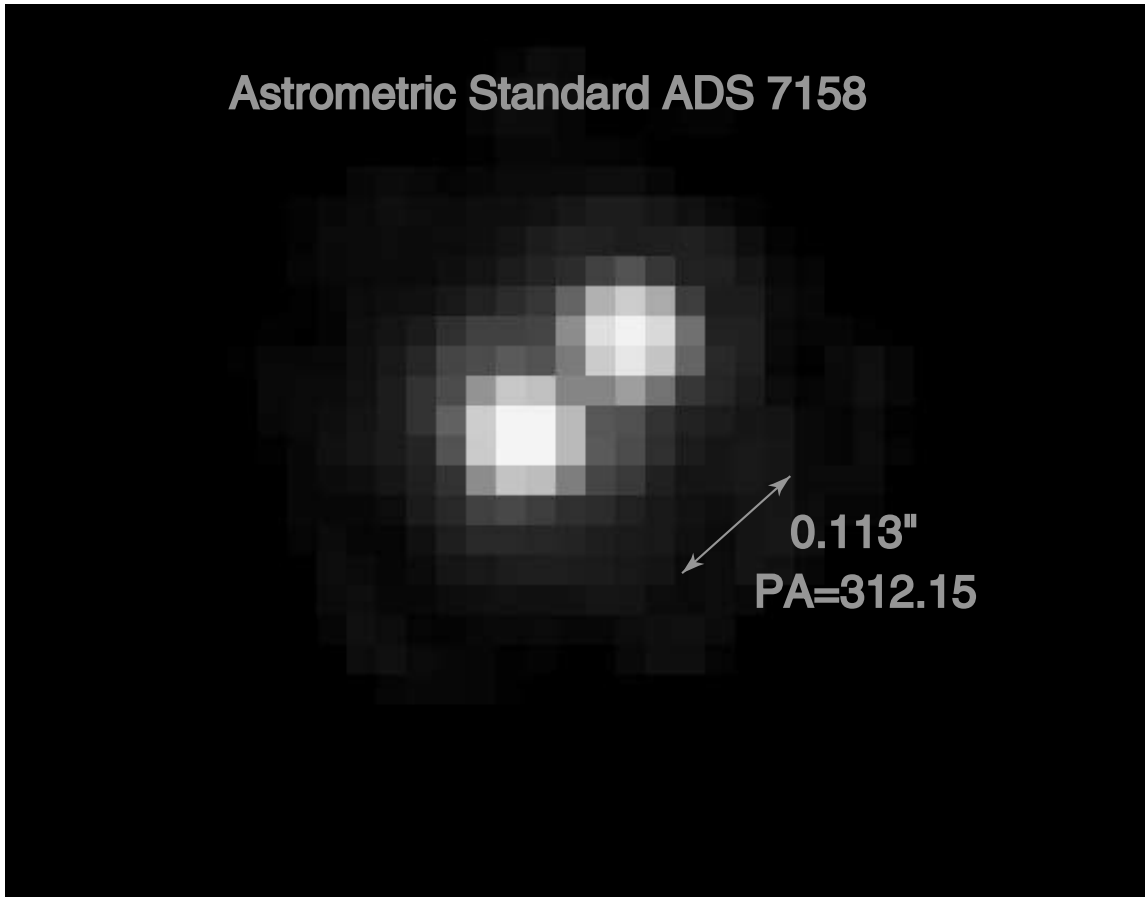


FIG. 3.—*H*-band image of the astrometric binary ADS 7158 (WDS 09036+4709; A1585). The well-known orbit (WDS grade level 2) of this binary star predicted a separation of  $0''.111$  and a P.A. of  $312^\circ.764$  for 2003 January 20 UT (the night of this observation). We utilized these values to check the  $0''.0242$   $\text{pixel}^{-1}$  plate scale and orientation (north being  $0^\circ.113$  east of the Indigo's *Y*-axis) that were obtained from the ADS 8939 observations for the Indigo camera (see Fig. 2). The above 10 s integration had a midpoint time of 8:18:50 UT; hence, the parallactic angle during this exposure was  $-171^\circ.0$ . Rotating the image by  $-171^\circ.0$  (and correcting for the  $0^\circ.113$  misalignment of the *Y*-axis) resulted in a measured P.A. of  $312^\circ.146$ , which is incorrect by  $0^\circ.62$ . Hence, we conservatively estimate that our P.A. is calibrated to  $\pm 1^\circ$ . The separation of ADS 7158 is 4.677 pixels, suggesting a plate scale of  $0''.0241$   $\text{pixel}^{-1}$ . Hence, we estimate a conservative  $\pm 0''.002$  error in the Indigo plate scale of  $0''.0242$   $\text{pixel}^{-1}$ . Color scale is logarithmic; note the Airy rings around each component. North is up, and east is to the left. [See the electronic edition of the *Journal* for a color version of this figure.]

excellent (there is no detectable change in PSF morphology due to anisoplanatic effects inside the  $\theta^1$  Ori B group (Diolaiti et al. 2000).

Since the PSF model was so accurate and the data had such a high signal-to-noise ratio (and high resolution), it was possible for DAOPHOT to measure relative positions to within  $0''.003$ . We estimate this error based on the scatter of the  $\theta^1$  Ori B1-B2 separation (which should be very close to a constant, since the B1-B2 system has an orbital period of  $\sim 2000$  yr). The lack of any motion between B1 and B2 is also confirmed by Schertl et al. (2003). Our data are summarized in Table 1. Linear (weighted) fits to the data in Table 1 (Figs. 7–14) yield the velocities shown in Table 1. The overall error in the relative proper motions observed is  $\sim 0''.002$   $\text{yr}^{-1}$  in proper motion ( $\sim 4$   $\text{km s}^{-1}$ ).

#### 4. ANALYSIS

With these accuracies it is now possible to determine whether these stars in the  $\theta^1$  Ori B group are bound together or merely chance projections in this very crowded region. As can be seen from Table 1 and Figures 7–14, there is very little relative motion between any of the members of the  $\theta^1$

Ori B group. Therefore, it is possible that the group is physically bound together.

If we adopt the mass of each star from the Siess, Forestini, & Dougados (1997) and Bernasconi & Maeder (1996) tracks fitted by Weigelt et al. (1999), we find masses of B1  $\sim 7$ , B2  $\sim 3$ , B3  $\sim 2.5$ , B4  $\sim 0.2$ , B5  $\sim 7$ , A1  $\sim 20$ , A2  $\sim 4$ , and A3  $\sim 2.6 M_\odot$ . Based on these masses (which are similar to those adopted by Schertl et al. 2003), we can comment on whether the observed motions are less than the escape velocities expected for simple face-on circular orbits.

Our combination of high spatial resolution and high signal-to-noise ratios yields an error in the proper motions of only  $\sim 0''.002$   $\text{yr}^{-1}$  according to the scatter in the B1-B2 and B1-B3 systems (see Table 1). We have observed orbital motion in the very tight  $\theta^1$  Ori B2-B3 (see Fig. 10) and  $\theta^1$  Ori A1-A2 (see Fig. 12) systems, with 52 and 94 AU separations, respectively.

##### 4.1. Is the $\theta^1$ Ori B2-B3 System Physical?

The relative velocity in the  $\theta^1$  Ori B2-B3 system (in the plane of the sky) is  $\sim 4.2 \pm 2.1$   $\text{km s}^{-1}$  (mainly in the azimuthal direction; see Fig. 10). This is a reasonable  $V_{\text{tan}}$ , since an orbital velocity of  $\sim 6.7$   $\text{km s}^{-1}$  is expected from a face-on

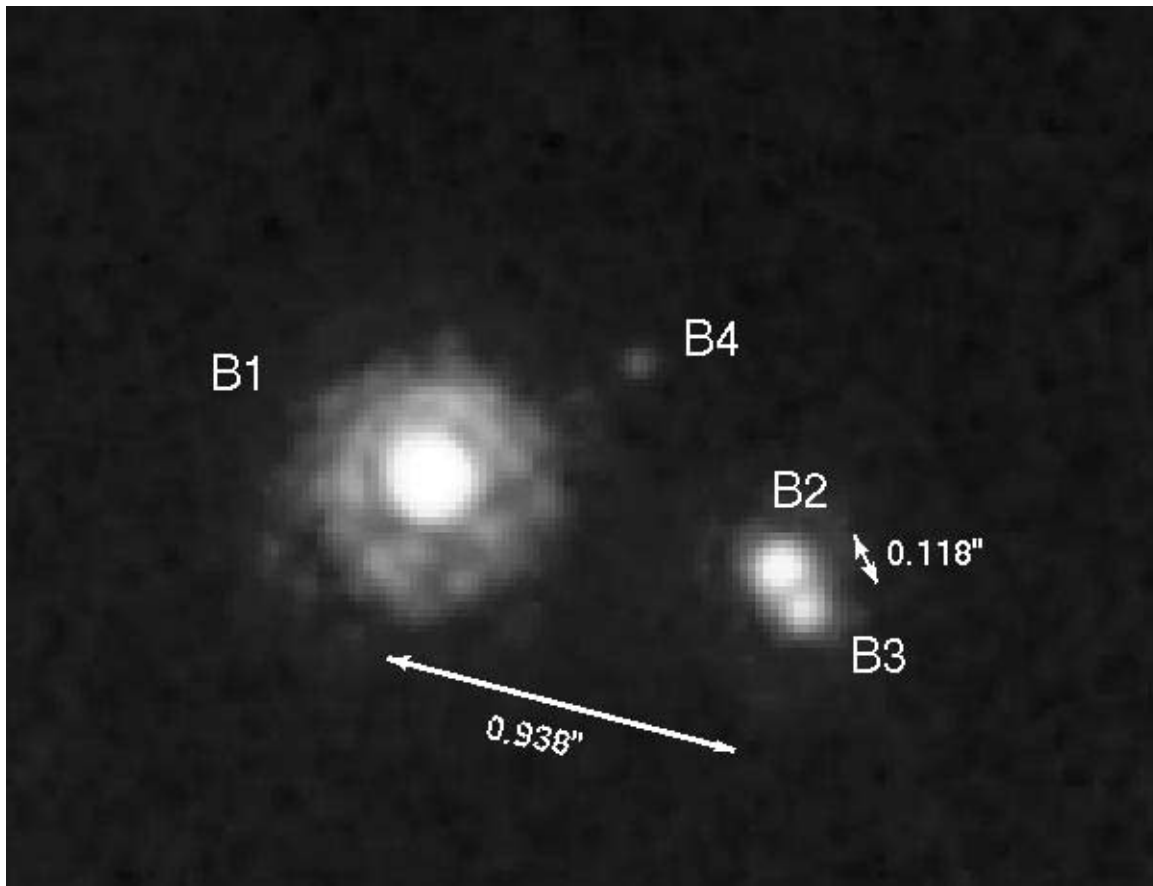


FIG. 4.—Detail of the  $\theta^1$  Ori B group as imaged at  $0''.077$  resolution (in the  $H$  band) with the MMT AO system and the Indigo IR camera. Color scale is logarithmic. North is up, and east is to the left. Note that the object “B1” is really an eclipsing spectroscopic binary (B1-B5), where the unseen companion B5 orbits B1 every 6.47 days (Abt et al. 1991). [See the electronic edition of the *Journal* for a color version of this figure.]

TABLE 1  
HIGH-RESOLUTION OBSERVATIONS OF THE  $\theta^1$  ORI B AND A GROUPS

System Name	$\Delta H$ (mag)	$\Delta K'$ (mag)	Separation (arcsec)	Separation Velocity (arcsec yr $^{-1}$ )	P.A. (deg)	P.A. Velocity (deg yr $^{-1}$ )	Telescope	Epoch
B1-B2.....	$2.30 \pm 0.15$		$0.942 \pm 0.020$	$-0.0006 \pm 0.0019$	$254.9 \pm 1.0$	$0.07 \pm 0.25$	SAO <sup>a</sup>	1997 Oct 14
		$1.31 \pm 0.10^b$	$0.942 \pm 0.020$		$254.4 \pm 1.0$		SAO <sup>a</sup>	1998 Nov 3
	$2.24 \pm 0.05$	$2.07 \pm 0.05$	$0.9388 \pm 0.0040$	$0.0006 \pm 0.0010$	$255.1 \pm 1.0$	$0.93 \pm 0.49$	GEMINI	2001 Sep 19
			$0.9375 \pm 0.0030$		$255.1 \pm 1.0$		MMT	2003 Jan 20
B2-B3.....	$1.00 \pm 0.11$		$0.114 \pm 0.05$	$-0.0017 \pm 0.0033$	$204.3 \pm 4.0$	$0.18 \pm 0.95$	SAO <sup>a</sup>	1997 Oct 14
		$1.24 \pm 0.20$	$0.117 \pm 0.005$		$205.7 \pm 4.0$		SAO <sup>a</sup>	1998 Nov 3
	$0.85 \pm 0.05$	$1.04 \pm 0.05$	$0.1166 \pm 0.0040$	$-0.0064 \pm 0.0027$	$207.8 \pm 1.0$	$2.13 \pm 0.73$	GEMINI	2001 Sep 19
			$0.1182 \pm 0.0030$		$209.7 \pm 1.0$		MMT	2003 Jan 20
B1-B4.....	$4.98 \pm 0.10$	$5.05 \pm 0.8$	$0.609 \pm 0.008$	$-0.0064 \pm 0.0027$	$298.0 \pm 2.0$		SAO <sup>c</sup>	2001 Feb 7
		$5.01 \pm 0.10$	$0.6126 \pm 0.0040$		$298.2 \pm 1.0$		GEMINI	2001 Sep 19
			$0.6090 \pm 0.0050$		$298.4 \pm 1.0$		MMT	2003 Jan 20
A1-A2.....	$1.51 \pm 0.15$		$0.208 \pm 0.030$	$-0.0064 \pm 0.0027$	$343.5 \pm 5.0$		Calar Alto <sup>d</sup>	1994 Nov 15
		$1.51 \pm 0.05$	$0.2215 \pm 0.005$		$353.8 \pm 2.0$		SAO <sup>a</sup>	1998 Nov 3
		$1.62 \pm 0.05$	$0.2051 \pm 0.0030$		$356.9 \pm 1.0$		GEMINI	2001 Sep 19

<sup>a</sup> Speckle observations of Weigelt et al. 1999.

<sup>b</sup> These low  $\Delta K'$  values are possibly due to  $\theta^1$  Ori B1 being in eclipse during the 1998 November 3 observations of Weigelt et al. 1999.

<sup>c</sup> Speckle observations of Schertl et al. 2003.

<sup>d</sup> Speckle observations of Petr et al. 1998.

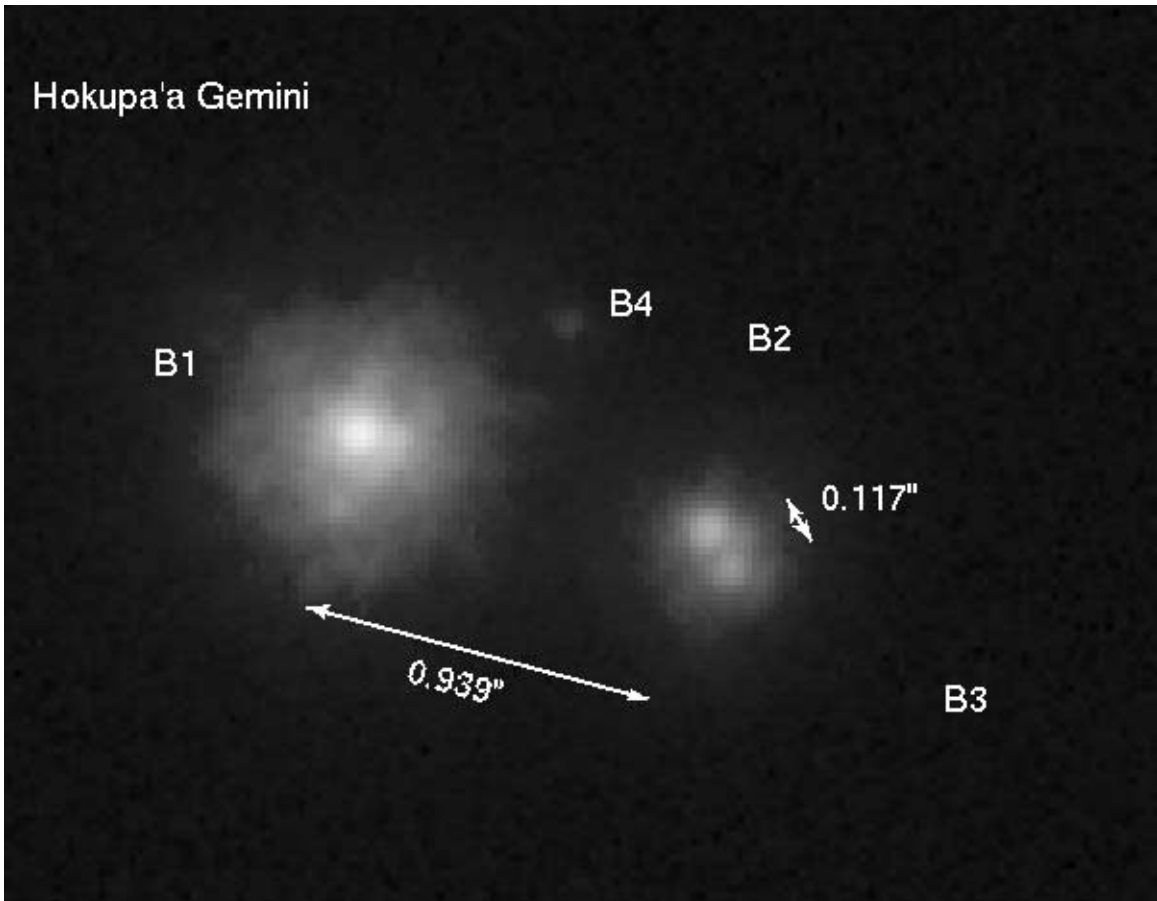


FIG. 5.—Gemini/Hokupa'a images of the  $\theta^1$  Ori B group in the  $K'$  band. Resolution is  $0''.085$ . Color scale is logarithmic. North is up, and east is to the left. [See the electronic edition of the *Journal* for a color version of this figure.]

circular orbit from a  $\sim 5.5 M_{\odot}$  binary system like  $\theta^1$  Ori B2-B3 with a 52 AU projected separation. It is worth noting that this velocity is also greater than the  $\sim 3 \text{ km s}^{-1}$  (Hillenbrand & Hartmann 1998) dispersion velocity of the cluster. Hence, it is most likely that these two  $K' = 7.6$  and  $8.6$  stars (separated by just  $0''.116$ ) are indeed in orbit around each other. Moreover, since there are only 10 stars known to have  $K' < 8.6$  in the inner  $30'' \times 30''$  (see Fig. 6), we can estimate that the chances of finding two bright ( $K' < 8.6$ ) stars within  $0''.116$  is a small, less than  $10^{-4}$  probability.

Our observed velocity of  $0''.93 \pm 0''.49 \text{ yr}^{-1}$  is consistent (in both direction and magnitude) with the  $1''.4 \text{ yr}^{-1}$  observed by Schertl et al. (2003). This suggests that the AO and speckle data sets are both detecting real motion. However, it will require a few more years of observation before an “arc” can be distinguished from linear motion.

#### 4.2. Is the $\theta^1$ Ori A1-A2 System Physical?

We observe  $\sim 16.5 \pm 5.7 \text{ km s}^{-1}$  of relative motion in the  $\theta^1$  Ori A1-A2 system (mainly in the azimuthal direction; see Fig. 12). This is higher than the average dispersion velocity of  $\sim 3 \text{ km s}^{-1}$  but still close to an estimated periastron velocity of the  $\sim 20 M_{\odot}$  A1- A2 system (projected separation of 94 AU). Hence, it is highly likely that these two  $K' = 6.0$  and  $7.6$  stars (separated by just  $0''.21$ ) are indeed in orbit around each other. In addition, since there are only eight stars known to have  $K' < 7.6$  in the inner  $30'' \times 30''$  (see Fig.

6), we can estimate that the chances of finding two bright ( $K' < 8.6$ ) stars within  $0''.21$  is a small, less than  $4 \times 10^{-4}$  probability.

Our observed velocity of  $16.5 \pm 5.7 \text{ km s}^{-1}$  is consistent (in both direction and magnitude) with the  $\sim 10.3 \text{ km s}^{-1}$  observed by Schertl et al. (2003). This again suggests that the AO and speckle data sets are both detecting real motion of A2 orbiting A1.

#### 4.3. Is the $\theta^1$ Ori B Group Stable?

The pair B1-B5 is moving at  $\sim 1.4 \pm 4.4 \text{ km s}^{-1}$  in the plane of the sky with respect to the pair B2-B3, where the escape velocity  $V_{\text{esc}} \sim 6 \text{ km s}^{-1}$  for this system. Hence, these pairs are very likely gravitationally bound together. However, radial velocity measurements will be required to be absolutely sure that these two pairs are bound together.

##### 4.3.1. Is the Orbit of $\theta^1$ Ori B4 Stable?

The situation is somewhat different for the faintest component of the group, B4. It has  $K' = 11.66$  mag, which, according to Hillenbrand & Carpenter (2000), suggests a mass of only  $\sim 0.2 M_{\odot}$ . Since there are only 20 stars known to have  $K' < 11.66$  in the inner  $30'' \times 30''$  (see Fig. 6), we can estimate that the chances of finding a  $K' < 11.66$  star within  $0''.6$  of B1 is a small, less than  $8 \times 10^{-3}$  probability. Our two AO measurements (and the one speckle detection of Schertl et al. 2003) did not detect a significant velocity of

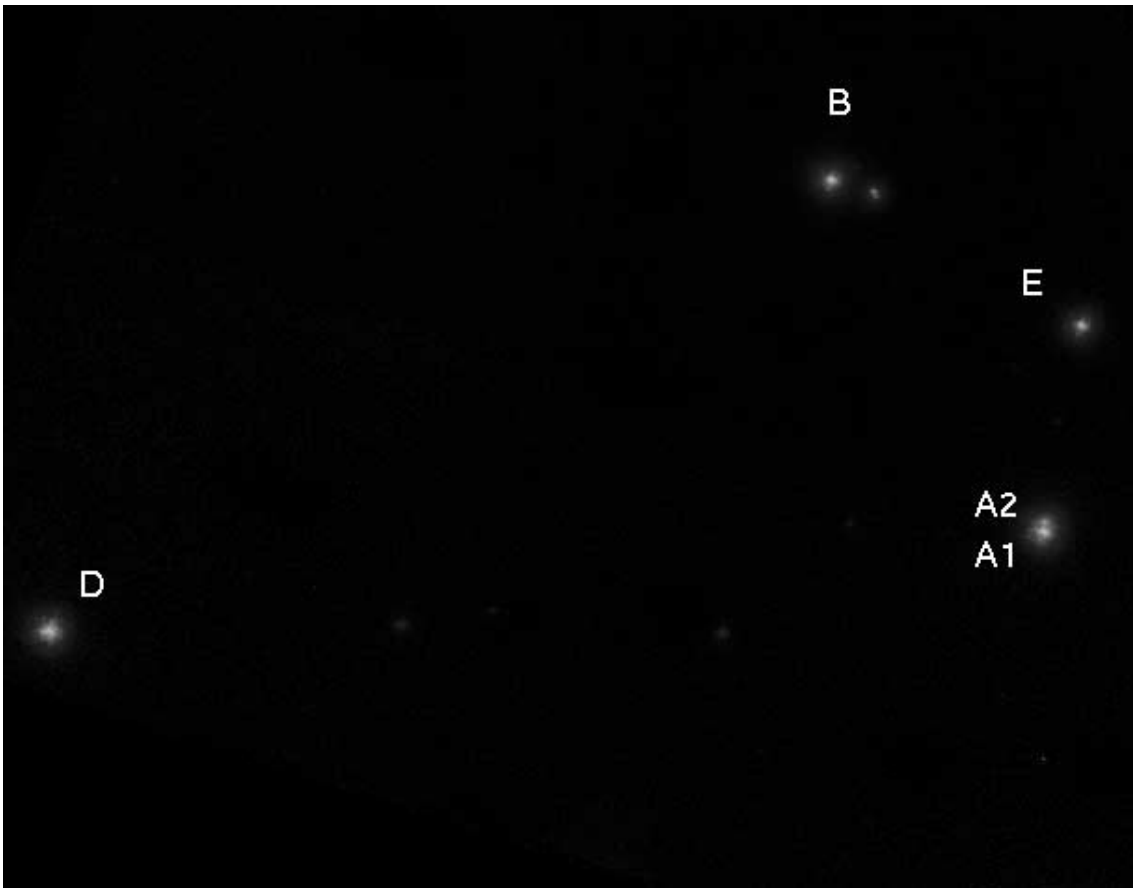


Fig. 6.—Upper part of the  $\theta^1$  Ori cluster as imaged over  $30'' \times 30''$  FOV at Gemini with the Hokupa'a AO system. Color scale is logarithmic. North is up, and east is to the left. Note that the object “A1” is really a spectroscopic binary (A1-A3), where the unseen companion A3 is separated from A1 by 1 AU (Bossi et al. 1989). [See the electronic edition of the Journal for a color version of this figure.]

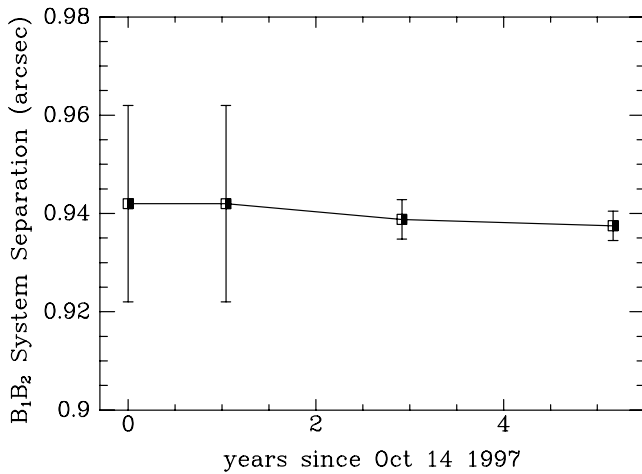


Fig. 7.—Separation between  $\theta^1$  Ori B1 and B2. Note how over 5 yr of observation there has been little significant relative proper motion observed ( $-0''.0006 \pm 0''.0019 \text{ yr}^{-1}$ , which is insignificantly different from a constant). If the group is gravitationally bound, the separation should be roughly constant over 5 yr. The observed rms scatter from a constant value is indeed a mere  $\pm 0''.0019$ , suggesting the whole  $\theta^1$  Ori B group is likely physically bound together. The first two data points are speckle observations from the 6 m SAO telescope (Weigelt et al. 1999), the next point is from our Gemini/Hokupa'a observations, and the latest data point is from the MMT AO observations.

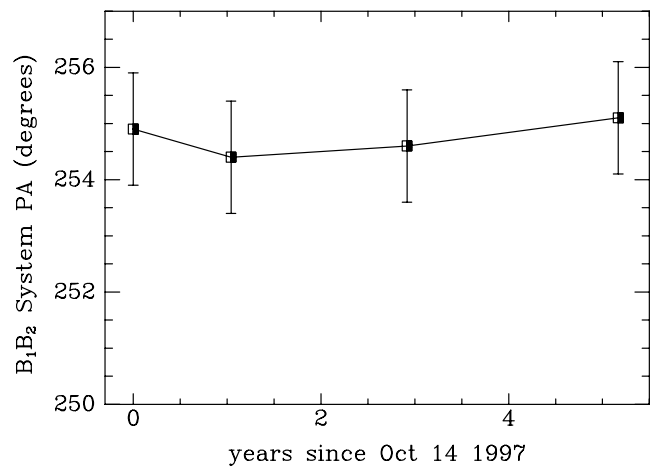


Fig. 8.—Position angle between  $\theta^1$  Ori B1 and B2. Note how over 5 yr of observation there has been no significant relative proper motion observed ( $0''.07 \pm 0''.25 \text{ yr}^{-1}$ , which is insignificantly different from a constant). The error from a constant value is a mere  $\pm 0''.3$ . The first two data points are speckle observations from the 6 m SAO telescope (Weigelt et al. 1999), the next point is from our Gemini/Hokupa'a observations, and the last data point is from the MMT AO observations.

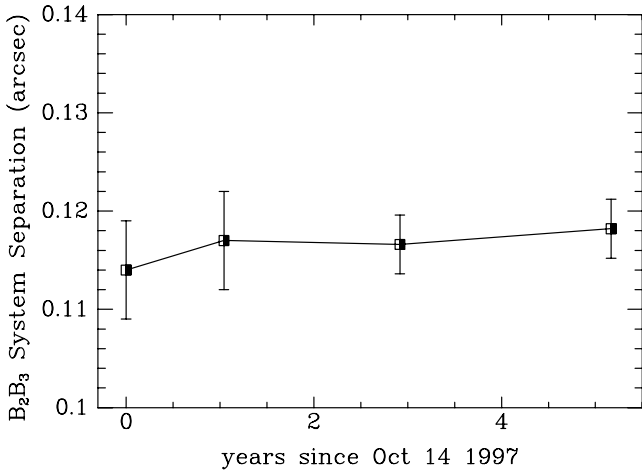


FIG. 9.—Separation between  $\theta^1$  Ori B2 and B3. Note the lack of any significant relative motion ( $0''.0006 \pm 0''.0010 \text{ yr}^{-1}$ ). The rms scatter from a constant value is only  $0''.001$ . There appears to very little change in the separation of the B2-B3 system. The first two data points are speckle observations from the 6 m SAO telescope (Weigelt et al. 1999), the next point is from our Gemini/Hokupa'a observations, and the last data point is from the MMT AO observations.

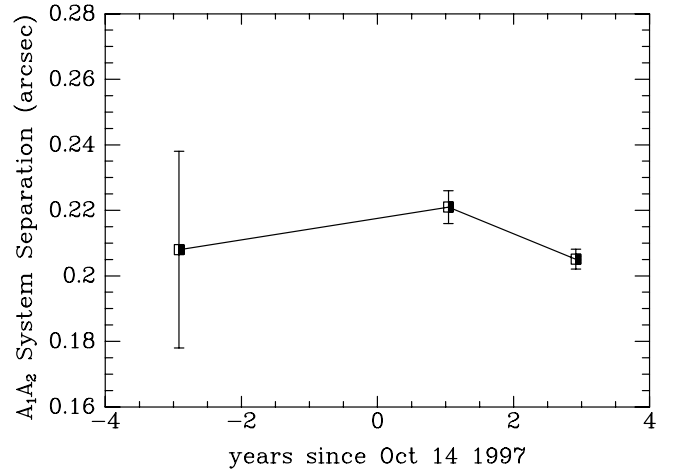


FIG. 11.—Separation between  $\theta^1$  Ori A1 and A2. There is a small negative change in the orbital separation ( $-0''.0064 \pm 0''.0027 \text{ yr}^{-1}$ ) as A2 moves toward A1. The first data point is from speckle observations at the 3.5 m Calar Alto telescope (Petr et al. 1998), the next point is from a speckle observation from the 6 m SAO telescope (Weigelt et al. 1999), and the last point is from our Gemini/Hokupa'a observations.

B4 with respect to B1 ( $4 \pm 15 \text{ km s}^{-1}$ ; see Figs. 13 and 14). Together with the escape velocity of  $\sim 6 \text{ km s}^{-1}$ , this points toward B4 also being a gravitationally bound member of the  $\theta^1$  Ori B group.

On the other hand, its mass and its location with respect to the other four group members makes it highly unlikely that B4 is on a stable orbit within the group. To reconcile these conflicting observations, one may think of (1) B4's projected distances from the other B group members being considerably smaller than the true distance, thus making a stable orbit much more likely; (2) B4's current motion pointing almost exactly along our line of sight, allowing for a higher true velocity; or (3) B4 being a chance projection of an object not related to the other four members of the B

group. Without additional astrometric data, we cannot yet decide which of these three possibilities is the most likely.

4.3.2. *Is the Orbit of B3 around B2 and of B5 around B1 Stable Long-Term?*

B1-B5, and B2-B3 are two binaries with projected separations of 0.13 AU (B1-B5) and 52 AU (B2-B3), respectively. The two pairs are separated by a projected distance of 415 AU. The distance  $D_{B1-B5} \sim 3 \times 10^{-4} \times D_{B1-B5-B2-B3}$ , and thus the B1-B5 system is stable. Much more interesting is the case of B2-B3. Their projected distance is not very small compared to their projected distance ( $D$ ) from the B1-B5 pair:  $D_{B2-B3} \sim 0.12 \times D_{B1-B5-B2-B3}$ . Thus, the stability of the

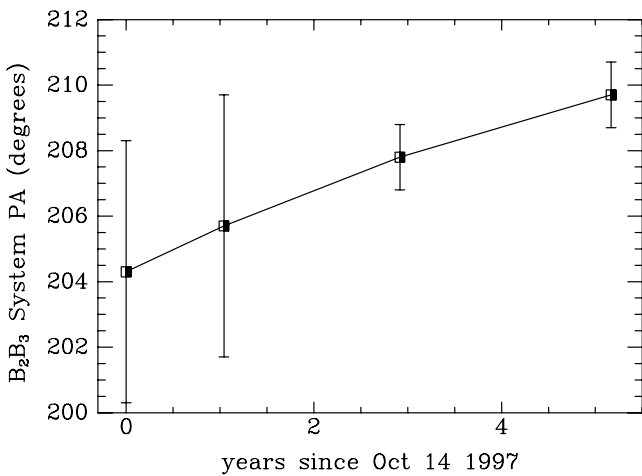


FIG. 10.—Position angle of  $\theta^1$  Ori B2 and B3. Here we observe what may be real orbital motion of B3 moving counterclockwise (at  $0''.93 \pm 0''.49 \text{ yr}^{-1}$ ; correlation significant at the 99.2% level) around B2. This small amount of motion is consistent with the B2-B3 system being bound. The first two data points are speckle observations from the 6 m SAO telescope (Weigelt et al. 1999), the next point is from our Gemini/Hokupa'a observations, and the last data point is from the MMT AO observations.

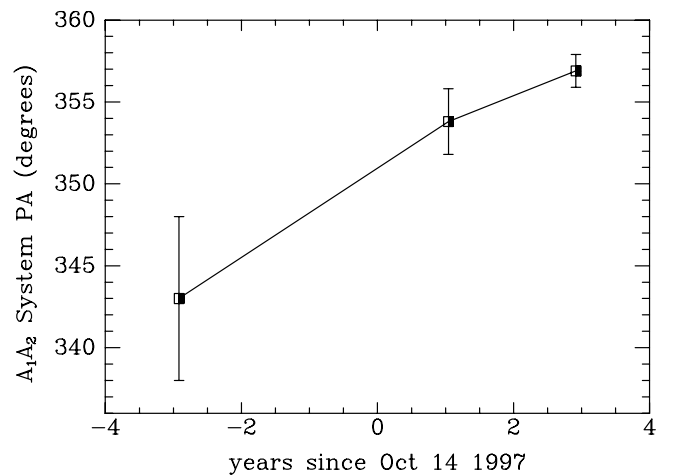


FIG. 12.—Position angle of  $\theta^1$  Ori A1 and A2. There do appear to be significant changes in the position angle as A2 moves counterclockwise (at  $2''.13 \pm 0''.73 \text{ yr}^{-1}$ ) around A1. This relatively small motion is consistent with the A1-A2 system being bound. The first data point is from speckle observations at the 3.5 m Calar Alto telescope (Petr et al. 1998), the next point is from a speckle observation from the 6 m SAO telescope (Weigelt et al. 1999), and the last point is from our Gemini/Hokupa'a observations.

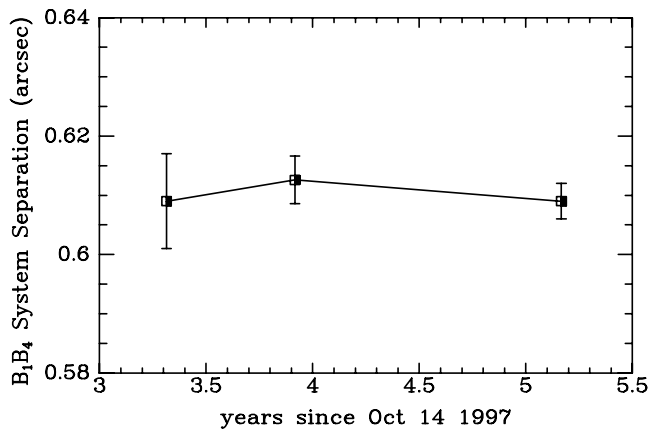


FIG. 13.—Separation between  $\theta^1$  Ori B1 and B4. Note how over 3 yr of observation there has been little significant relative proper motion observed ( $-0''.0017 \pm 0''.0033 \text{ yr}^{-1}$ , which is insignificantly different from a constant). If the low-mass star B4 is gravitationally bound to the B group, the B1-B4 separation should be roughly constant over these 3 yr. The observed rms scatter from a constant value is indeed a mere  $\pm 0''.0033$ , suggesting B4 is bound to the  $\theta^1$  Ori B group. The first data point is a speckle observation from the 6 m SAO telescope (Schertl et al. 2003), the next point is from our Gemini/Hokupa'a observations, and the last data point is from the MMT AO observations.

B2-B3 orbit needs a more detailed analysis, since it is possible that B3 may be ejected in the future.

Eggleton & Kiseleva (1995) have given an empirical criterion for the long-term stability of the orbits of hierarchical triple systems, based on the results of their extensive model calculations (Kiseleva, Eggleton, & Ansova 1994a; Kiseleva, Eggleton, & Orlov 1994b; Eggleton & Kiseleva 1995). Their analytic stability criterion is good to about  $\pm 20\%$  and is meant to indicate stability for another  $10^2$  orbits. Given the uncertainties of the masses of the members of the B group, this accuracy is sufficient for our present discussion.

The orbital period of the two binaries with respect to each other is  $P_{(1,5)/(2,3)} \sim 1920$  yr, while the orbital period of B3 with respect to B2 amounts to  $P_{2/3} \sim 160$  yr. For the calculation of both periods, we have assumed the masses as given above and circular orbits in the plane of the sky. This leads to a period ratio  $X = P_{(1,5)/(2,3)}/P_{2/3} \sim 12$ . Eggleton & Kiseleva's stability criterion requires  $X \geq X_{\text{crit}} = 10.08$  for the masses in the B group. This means that within the accuracy limits of our investigation, the binary B2-B3 is just at the limit of stability. The stability criterion also depends on the orbits' eccentricities. In our case, already mild eccentricities of the order of  $e \sim 0.1$  (as can be expected to develop in hierarchical triple systems; see, e.g., Georgakarakos 2002) make the B group unstable. While we cannot decide yet whether the pair B2-B3 orbit each other in a stable way, it is safe to say that the "triple" B1-B5, B2, and B3 is not a simple, stable hierarchical triple system.

The  $\theta^1$  Ori B system seems to be a good example of a highly dynamic star formation minicluster that is possibly in the process of ejecting the lowest mass member through dynamical decay (Durisen et al. 2001) and breaking up the gravitational binding of the widest of the close binaries (the B2-B3 system). The ejection of the lowest mass member of a formation minicluster could play a major role in the formation of low-mass stars and brown dwarfs (Reid et al. 2001; Bate et al. 2002; Durisen et al. 2001; Close et al. 2003a). The

breaking up of binaries, of course, modifies the binary fraction of main-sequence stars considerably as well.

## 5. FUTURE OBSERVATIONS

In our opinion it is most likely that these  $\theta^1$  Ori A and B group stars are bound. We caution, however, that the motion of each of these stars could currently be fitted equally well by linear motion (not orbital arcs). Future high-resolution observations are required to see whether these stars follow true orbital arcs around each other, proving that they are interacting. In particular, future observations of the  $\theta^1$  Ori B4 positions would help reduce the scatter in the velocity data and indicate whether it is indeed part of the  $\theta^1$  Ori B group.

Future observations should also try to determine the radial velocities of these stars. Once radial velocities are known, one can calculate unambiguously whether these systems are bound. Such observations will require both very high spatial and spectral resolutions. This might be possible with such future instruments as the future AO-fed ARIES instrument.

These MMT observations could not have been possible without the hard work of the entire Center for Astronomical Adaptive Optics (CAAO) staff at the University of Arizona. In particular, we would like to thank Tom McMahon, Kim Chapman, Doris Tucker, and Sherry Weber for their endless support of this project. The adaptive secondary mirror is a joint project of University of Arizona and the Italian National Institute of Astrophysics-Arcetri Observatory. We would also like thank the whole MMT staff for their excellent support and flexibility during our commissioning run at the telescope. The Hokupa'a AO observations were supported by the University of Hawaii AO group. (D. Potter, O. Guyon, and P. Baudoz). Support for Hokupa'a comes from the National Science Foundation. These results were based, in part, on observations obtained at the Gemini Observatory, which is operated by the Association of Universities for Research in Astronomy, Inc., under a cooperative agreement with the NSF on behalf of the Gemini

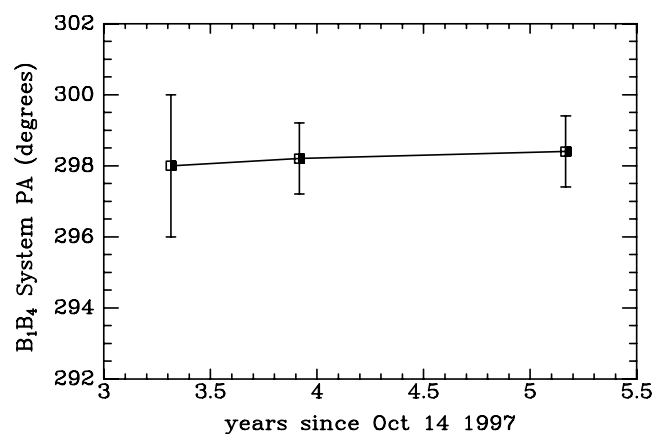


FIG. 14.—Position angle between  $\theta^1$  Ori B1 and B4. Note how over 3 yr of observation there has been no significant relative proper motion observed ( $0''.18 \pm 0''.9 \text{ yr}^{-1}$ , which is insignificantly different from a constant). The first data point is a speckle observation from the 6 m SAO telescope (Schertl et al. 2003), the next point is from our Gemini/Hokupa'a observations, and the last data point is from the MMT AO observations.

partnership: the National Science Foundation (United States), the Particle Physics and Astronomy Research Council (United Kingdom), the National Research Council (Canada), CONICYT (Chile), the Australian Research Council (Australia), CNPq (Brazil), and CONICET (Argentina). The secondary mirror development could not

have been possible without the support of the Air Force Office of Scientific Research under grant AFOSR F49620-00-1-0294. L. M. C. acknowledges support from NASA Origins grant NAG5-12086 and NSF SAA grant AST 02-06351.

## REFERENCES

- Abt, H. A., Wang, R., & Cardona, O. 1991, *ApJ*, 367, 155  
 Bate, M. R., Bonnell, I. A., & Bromm, V. 2002, *MNRAS*, 332, L65  
 Bernasconi, P. A., & Maeder, A. 1996, *A&A*, 307, 829  
 Biller, B., et al. 2003, *ApJ*, submitted  
 Bossi, M., Gaspani, A., Scardia, M., & Tadini, M. 1989, *A&A*, 222, 117  
 Bouy, H., Brandner, W., Martín, E., Delfosse, X., Allard, F., & Basri, G. 2003, *AJ*, 126, 1526  
 Brusa, G., et al. 2003, *Proc. SPIE*, in press  
 Burgasser, A., et al. 2003a, *ApJ*, 586, 512  
 Close, L. M. 2000, *Proc. SPIE*, 4007, 758  
 ———. 2003, *Proc. SPIE*, 4834, 84  
 Close, L. M., Roddier, F. J., Roddier, C. A., Graves, J. E., Northcott, M. J., & Potter, D. 1998, *Proc. SPIE*, 3353, 406  
 Close, L. M., Siegler, N., Freed, M., & Biller, B. 2003a, *ApJ*, 587, 407  
 Close, L. M., et al. 2002a, *ApJ*, 566, 1095  
 ———. 2002b, *ApJ*, 567, L53  
 ———. 2003b, *ApJ*, 598, L35  
 Diolaiti, E., Bendinelli, O., Bonaccini, D., Close, L., Currie, D., & Parmeggiani, G. 2000, *A&AS*, 147, 335  
 Duquennoy, A., & Mayor, M. 1991, *A&A*, 248, 485  
 Durisen, R. H., Sterzik, M. F., & Pickett, B. K. 2001, *A&A*, 371, 952  
 Eggleton, P., & Kiseleva, L. 1995, *ApJ*, 455, 640  
 Genzel, R., & Stutzki, J. 1989, *ARA&A*, 27, 41  
 Georgakarakos, N. 2002, *MNRAS*, 337, 559  
 Gizis, J. E., et al. 2003, *AJ*, 125, 3302  
 Graves, J. E., Northcott, M. J., Roddier, F. J., Roddier, C. A., & Close, L. M. 1998, *Proc. SPIE*, 3353, 34  
 Hillenbrand, L. A., & Carpenter, J. 2000, *ApJ*, 540, 236  
 Hillenbrand, L. A., & Hartmann, L. W. 1998, *ApJ*, 492, 540  
 Hinz, J. L., McCarthy, D. W., Simons, D. A., Henry, T. J., Kirkpatrick, J. D., & McGuire, P. C. 2002, *AJ*, 123, 2027  
 Hodapp, K.-W., et al. 1996, *NewA*, 1, 177  
 Kiseleva, L. G., Eggleton, P. P., & Anosova, J. P. 1994a, *MNRAS*, 267, 161  
 Kiseleva, L. G., Eggleton, P. P., & Orlov, V. V. 1994b, *MNRAS*, 270, 936  
 Lloyd-Hart, M. 2000, *PASP*, 112, 264  
 McCarthy, C., Zuckerman, B., & Becklin, E. E. 2003, in *IAU Symp.* 211, *Brown Dwarfs*, ed. E. Martín (San Francisco: ASP), 279  
 McCarthy, D. W., et al. 1998, *Proc. SPIE*, 3354, 750  
 McCaughrean, M. J., & Stauffer, J. R. 1994, *AJ*, 108, 1382  
 Petr, M. G., Du Foresto, V., Beckwith, S. V. W., Richichi, A., & McCaughrean, M. J. 1998, *ApJ*, 500, 825  
 Potter, D., et al. 2002a, *ApJ*, 567, L133  
 Reid, I. N., Gizis, J. E., Kirkpatrick, J. D., & Koerner, D. W. 2001, *AJ*, 121, 489  
 Reipurth, B., & Clarke, C. 2001, *AJ*, 122, 432  
 Schertl, D., Balega, Y. Y., Preibisch, Th., & Weigelt, G. 2003, *A&A*, 402, 267  
 Siegler, N., Close, L. M., & Freed, M. 2003, *Proc. SPIE*, 4839, 114  
 Siess, L., Forestini, M., & Dougados, C. 1997, *A&A*, 324, 556  
 Simon, M., Close, L. M., & Beck, T. 1999, *AJ*, 117, 1375  
 Stetson, P. B. 1987, *PASP*, 99, 191  
 Weigelt, G., Balega, Y., Preibisch, T., Schertl, D., Scholler, M., & Zinnecker, H. 1999, *A&A*, 347, L15  
 Wildi, F., Brusa, G., Riccardi, A., Lloyd-Hart, M., Martin, H. M., & Close, L. M. 2003a, *Proc. SPIE*, 4839, 155  
 Wildi, F., et al. 2003b, *Proc. SPIE*, in press